ORIGINAL ARTICLE

Cancer Science WILEY

Oncogenic splicing abnormalities induced by *DEAD-Box Helicase 56* amplification in colorectal cancer

Yuta Kouyama[1,2] | Takaaki Masuda[1] | Atsushi Fujii[1] | Yushi Ogawa[2] |
Kuniaki Sato[1] | Taro Tobo[3] | Hiroaki Wakiyama[1] | Yukihiro Yoshikawa[1] |
Miwa Noda[1] | Yusuke Tsuruda[1] | Yousuke Kuroda[1] | Hidetoshi Eguchi[1] |
Fumio Ishida[2] | Shin-ei Kudo[2] | Koshi Mimori[1] 🔟

[1]Department of Surgery, Kyushu University Beppu Hospital, Oita, Japan

[2]Digestive Disease Center, Showa University Northern Yokohama Hospital, Yokohama, Japan

[3]Department of Clinical Laboratory Medicine, Kyushu University Beppu Hospital, Oita, Japan

Correspondence
Koshi Mimori, Department of Surgery, Kyushu University Beppu Hospital, Beppu, Oita, Japan.
Email: kmimori@beppu.kyushu-u.ac.jp

Abstract

Alternative splicing, regulated by DEAD-Box Helicase (DDX) families, plays an important role in cancer. However, the relationship between the DDX family and cancer has not been fully elucidated. In the present study, we identified a candidate oncogene *DDX56* on Ch.7p by a bioinformatics approach using The Cancer Genome Atlas (TCGA) dataset of colorectal cancer (CRC). DDX56 expression was measured by RT-qPCR and immunochemical staining in 108 CRC patients. Clinicopathological and survival analyses were carried out using three CRC datasets. Biological roles of DDX56 were explored by gene set enrichment analysis (GSEA), and cell proliferation in vitro and in vivo, cell cycle assays, and using *DDX56*-knockdown or overexpressed CRC cells. RNA sequencing was carried out to elucidate the effect of DDX56 on mRNA splicing. We found that DDX56 expression was positively correlated with the amplification of DDX56 and was upregulated in CRC cells. High DDX56 expression was associated with lymphatic invasion and distant metastasis and was an independent poor prognostic factor. In vitro analysis, in vivo analysis and GSEA showed that DDX56 promoted proliferation ability through regulating the cell cycle. *DDX56* knockdown reduced intron retention and tumor suppressor WEE1 expression, which functions as a G2-M DNA damage checkpoint. We have identified *DDX56* as a novel oncogene and prognostic biomarker of CRC that promotes alternative splicing of WEE1.

KEYWORDS
biomarker, colorectal cancer, DEAD-Box Helicase 56 (DDX56), oncogene, splicing factor

1 | INTRODUCTION

RNA splicing is the process of generating a mature mRNA from pre-mRNA, during which exon-intron borders are recognized and the intervening intronic sequences are removed.[1,2] RNA splicing enables the production of multiple mRNA species by alternative splicing of exons, which are found in nearly 95% of mammalian genes, to generate tissue- and species-specific differentiation patterns.[1,3]

Deregulated or abnormal splicing is often observed in various malignancies, including colorectal cancer (CRC), which is one of the most common malignant tumors worldwide.[4-6] Furthermore, splicing abnormality has recently been recognized as an important mechanism for regulating the expression of cancer-related genes.[5-10]

In CRC and colorectal adenoma, amplification of chromosome 7p (Ch.7p) occurs frequently.[11-13] Recently, our multiregional genomic analysis showed that the amplification of Ch.7p occurs in all regions of an individual tumor.[14-16] These data suggest that the amplification of Ch.7p is a fundamental and predominant event in tumorigenesis of CRC, and that Ch.7p harbors driver genes that promote tumorigenesis or tumor progression through gain of function as a result of genomic amplification. Moreover, these driver genes on Ch.7p could be an optimal therapeutic target to overcome intratumor heterogeneity, which is considered to be a major cause of treatment resistance.[17]

We carried out oncogene screening using a bioinformatics approach to analyze population data and compare gene expression between tumors and normal tissues, and to examine the correlation between chromosomal copy number and gene expression. Using this screening approach, we previously identified phosphoserine phosphatase (*PSPH*), located on Ch.7p, as a driver gene in CRC.[11]

Herein, we used our screening method and identified DEAD-Box helicase (DDX56), as a candidate oncogene. *DDX56* is located on Ch.7p and is a member of the DDX family, known to regulate alternative splicing.[18-20] Furthermore, using in vitro and in vivo experiments and RNA sequencing analysis, we determined the clinicopathological and oncogenic features of DDX56 in CRC, and confirmed splicing alteration as the oncogenic mechanism of action.

2 | MATERIALS AND METHODS

2.1 | Kyushu dataset

A total of 108 patients with CRC who underwent surgical resection of a primary tumor at Kyushu University Beppu Hospital and affiliated hospitals between 1992 and 2007 were enrolled in this study. Clinicopathological factors and clinical stage were classified using the TNM system of classification. All patients were treated in accordance with the Japanese Society of Cancer of the Colon and Rectum Guidelines for the Treatment of Colorectal Cancer.[21] Written informed consent was obtained from all patients. Resected tumor tissues and paired normal colon tissues were immediately stored in RNAlater (Ambion), frozen in liquid nitrogen and kept at −80°C until RNA extraction. All protocols used in this study were approved by the local ethics review board of Kyushu University.

2.2 | Public datasets

We obtained RNA sequencing data of all cancer types, DNA copy number data, mutation annotation file, intron expression data, and clinical assessments of CRC patients in TCGA from the Broad Institute's Firehose (http://gdac.broadinstitute.org) as a TCGA dataset. mRNA expression (raw count and Fragments Per Kilobase of transcript per Million mapped reads [FPKM]) data were normalized with quantile normalization. The GSE21815 dataset was downloaded from the Gene Expression Omnibus (GEO) database (https://www.ncbi.nlm.nih.gov/geo) as a GSE dataset. It contained mRNA expression and clinical data of 132 CRC patients in Japan. We obtained *DDX56* mRNA expression and DNA copy number data for 50 CRC cell lines from the Cancer Cell Line Encyclopedia (https://portals.broadinstitute.org/ccle/home) as a CCLE dataset.

2.3 | Selection of candidate genes

Using the TCGA dataset, we extracted candidate genes from 426 genes on Ch.7p that satisfied the following two criteria, as described previously:[11] (i) DNA copy number and mRNA expression levels were positively correlated with each other (correlation coefficient cut-off set at 4); (ii) the gene of interest was overexpressed in tumor tissues compared to normal tissues (>2-fold change). Genes selected using this strategy were found to be candidate driver genes in CRC, induced by Ch.7p amplification (Figure 1).

2.4 | Pan-cancer analysis

Raw count and quantile normalized mRNA data for all cancer types were obtained from TCGA dataset. Those cancer types that had less than 10 normal tissues for comparison were excluded from our analysis. mRNA expression in the following cancers was compared to mRNA expression in the respective non-cancerous tissues: bladder urothelial carcinoma (BLCA), breast invasive carcinoma (BRCA), head and neck squamous cell carcinoma (HNSC), pan-kidney cohort (KIPAN), liver hepatocellular carcinoma (LIHC), lung adenocarcinoma (LUAD), lung squamous cell carcinoma (LUSC), prostate adenocarcinoma (PRAD), and stomach and esophageal carcinoma (STES).
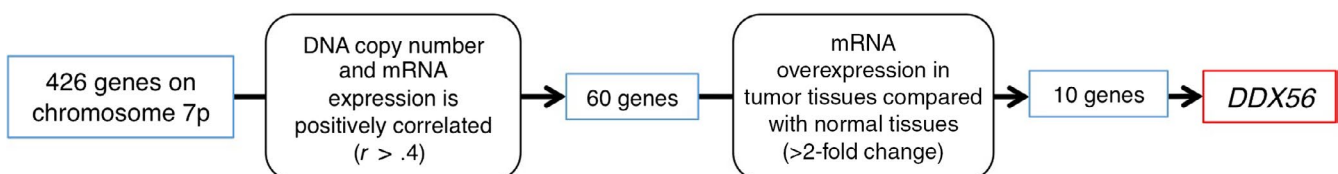
FIGURE 1 Schematic diagram of the strategy for selection of candidate genes in colorectal carcinoma

2.5 | Cell lines and cell culture

Human CRC cell lines CaR-1, Colo320, Colo201, LoVo, SW480, and DLD-1 were obtained from JCRB cell bank; Colo205 and HCT116 were obtained from RIKEN BioResource Research Center; and RKO, and SW620 were obtained from the ATCC. All cell lines were cultured in appropriate medium supplemented with 10% FBS at 37°C in an atmosphere containing 5% CO_2.

2.6 | RNA extraction and reverse transcription-quantitative polymerase chain reaction

RNA was extracted from frozen tissue specimens and cell lines using ISOGEN-II (Nippon Gene), and RT- quantitative polymerase chain reaction (qPCR) was carried out as previously described.[11] Gene expression was quantified using the following oligonucleotide primers: DEAD-box helicases (*DDX56*): 5′-GCAGCAAGACAGCCTGAAAC-3′ (sense) and 5′-GGGCAAGT GACAGAGGAGAC-3′ (antisense), *WEE1* intron: 5′-GCAGTGCTTG GACAGCATTCAC-3′ (sense) and 5′-TCTCAAGCTCACAAGAAAA CCA-3′ (antisense), *GAPDH*: 5′-AGCCACATCGCTCAGACAC-3′ (sense) and 5′-GCCCAATACGACCAAATCC-3′ (antisense), and 18s: 5′-AGTCCCTGCCCTTTGTACACA-3′ (sense) and 5′-CGATCCGAG GGCCTCACTA-3′ (antisense). Gene expression was normalized to *GAPDH* or 18s expression as an internal control in each sample.

2.7 | Immunohistochemical analysis

Immunohistochemistry of DDX56 in CRC tissues samples was carried out as previously described.[22] A mouse monoclonal anti-DDX56 antibody (H00054606-M05; Novus Biologicals) was used as the primary antibody diluted at 1:100. Tumor histology was independently reviewed by an experienced pathologist (T.T.).

2.8 | Knockdown analysis of DDX56 by siRNA

Knockdown analysis of *DDX56* was carried out with siRNAs (DDX56 siRNA-1; s29253 and DDX56 siRNA-2; s29254; Thermo Fisher Scientific) and Silencer Negative Control 1 siRNA (AM4611; Invitrogen). CaR-1 and LoVo cell lines were transfected with siRNA (10 nmol/L) using RNAiMAX (Invitrogen) according to the manufacturer's protocol.

2.9 | Knockdown analysis of DDX56 using shRNA

DDX56 human shRNA retroviral untagged vector plasmid (DDX56 Human shRNA Plasmid Kit) was obtained from OriGene Technologies. A control shRNA retroviral vector was also obtained from OriGene Technologies. Retrovirus was produced in 293T cells using Retrovirus Packaging Kit Ampho (TaKaRa) and the media collected after 48 hours for transduction of CaR-1 cells. Cells were transduced with retroviral supernatant and then selected with 2.5 μg/mL puromycin to generate cells with stable knockdown of DDX56.

2.10 | Overexpression analysis of DDX56

Overexpression analysis was carried out using plasmid clone of human DDX56 cDNA with CMV promoter (IRAK004D19; Riken BioResource Research Center). As a negative control, we used empty vector with CMV promoter (pcDNA 3.3-TOPO TA Cloning Kit; Invitrogen). We transfected the vectors for SW480 cells using Lipofectamine3000 (Invitrogen) following the manufacturer's protocol.

2.11 | Murine xenograft model

All animal procedures were carried out in compliance with the Guidelines for the Care and Use of Experimental Animals established by the Committee for Animal Experimentation of Kyushu University. Murine xenograft model analysis was conducted as described previously.[23] Five-week-old female BALB/cSlc nu/nu mice were purchased from Japan SLC, Inc. and maintained under specific pathogen-free conditions. For xenograft assays, 10^6 CaR-1 cells transfected with DDX56 shRNA or control RNA were suspended in 100 μL PBS and the cells bilaterally injected under the skin of four nude mice. Tumor sizes were measured 6, 7, 9, and 13 days after injection using a Vernier caliper and calculated using the following formula: tumor volume = length × width^2 × 0.5.

2.12 | Western blot analysis

Western blot analysis was carried out as previously described.[24] The following antibodies were used: primary rabbit polyclonal anti-DDX56 antibody (H00054606-M05; Novus Biologicals) at 1:200 dilution; anti-WEE1 N-terminal antibody (SAB4503088; Merck) at 1:200 dilution, and primary mouse polyclonal anti-β-actin antibody (Santa Cruz Biotechnology) at 1:200 dilution. Expression of DDX56 and WEE1 proteins were normalized to β-actin protein expression.

2.13 | MTT assay

Cell proliferation was evaluated by MTT assay (Roche Applied Science) according to the manufacturer's instructions, as described previously.[25] In brief, cells transfected with DDX56 siRNA and negative control siRNA transfected cells were seeded in triplicate at 10^4 cells/well in 100 μL medium in a 96-well plate. Color change was quantitated using an Immuno-Mini NJ-2300 automatic plate reader (Nihon InterMed) at 570 nm with a 650-nm reference filter.

2.14 | Colony formation assay

Cell growth was assessed using colony formation assay. Cells were seeded at 10^3 cells/well in 3 mL medium in 6-well plates and transfected with DDX56 siRNA or negative control siRNA. After 14 days, colonies were stained using Differential Quik Stain Kit (Sysmex) according to the manufacturer's instructions. Visible colonies were
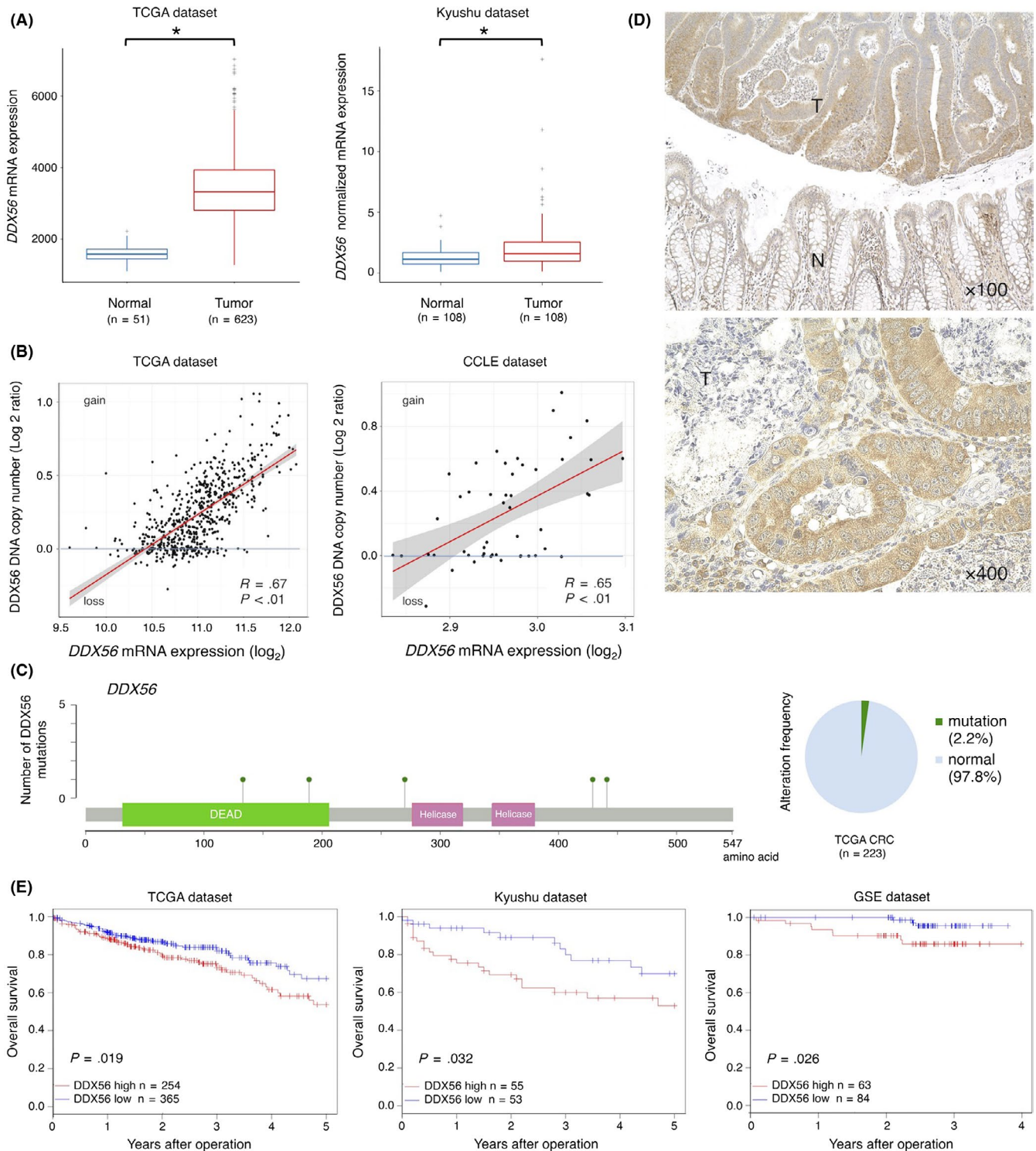
FIGURE 2 Clinical significance of DDX56 expression in colorectal carcinoma (CRC). A, *DDX56* mRNA expression in CRC tissues and normal colon tissues in The Cancer Genome Atlas (TCGA) dataset and Kyushu dataset. B, Correlation between DNA copy number and mRNA expression of DDX56 in TCGA dataset and Cancer Cell Line Encyclopedia (CCLE) dataset. *R* is the Pearson correlation coefficient. C, Positions and frequency of mutations in DDX56 among CRC cases in TCGA dataset. Number of mutations was observed in five cases and frequency was 2.2%. D, Immunohistochemical staining for DDX56 in CRC tissues and normal tissues. N, normal tissue; T, tumor tissue. E, Kaplan-Meier overall survival curves of patients with CRC according to *DDX56* mRNA expression in TCGA dataset (n = 619), Kyushu dataset (n = 108), and gene set enrichment (GSE) dataset (n = 147)

TABLE 1 Relationship between DDX56 expression and clinicopathological factors

Variable	High expression (n = 55)	Low expression (n = 53)	P-value
Age (y)			
Mean ± SD	67.5 ± 10.5	67.1 ± 11.4	.60
Gender			
Male	30	41	<.05
Female	25	12	
Tumor location			
Left	18	14	.53
Right	37	39	
Histology			
well/mod	49	50	.49
por/muc	6	3	
Tumor size (cm)			
mean ± SD	4.6 ± 2.0	4.9 ± 2.5	.69
T stage			
1, 2	14	16	.67
3, 4	41	37	
Lymphatic invasion			
−	25	37	<.01
+	30	16	
Vascular invasion			
−	39	40	.67
+	16	13	
Lymph node metastasis			
−	24	27	.56
+	31	26	
Distant metastasis			
−	43	49	<.05
+	12	4	
TNM stage			
I, II	29	24	.45
III, IV	26	29	

Data are expressed as the number of patients (%) unless otherwise indicated.

mod, moderately differentiated adenocarcinoma; muc, mucinous adenocarcinoma; por, poorly differentiated adenocarcinoma; SD, standard deviation; well, well-differentiated adenocarcinoma.

photographed using a Chemiluminescence Imaging FUSION Solo S (Vilber). Colony counts were determined using ImageJ software.

2.15 | Cell cycle assay

For cell synchronization, we used nocodazole (an inhibitor of tubulin assembly) as previously described.[26] Forty-eight hours after transfection, 5 µg/mL nocodazole was added to cells. Cells were incubated for 16 hours and then washed with PBS and harvested in normal medium at various timepoints (0, 6, 12, 18, 24 hours). Cells were washed with PBS and fixed in 70% ethanol at −20°C overnight. Samples were then washed with PBS and stained with propidium iodide (PI) (Wako, Inc.) containing RNase A for 20 minutes at 37°C. Cell cycle distribution was measured using FACS (SH800S Cell Sorter; Sony Biotechnology, Inc.). Cells were classified into G1/S/G2M phases, according to DNA content, and the relative ratio of cells in G1 and G2M phase was compared between DDX56 siRNA-transfected cells and control siRNA-transfected cells.

2.16 | RNA sequence

RNA-sequence (RNA-seq) was carried out using Illumina HiSeq 2500 by BGI. We sent total RNA transfected with DDX56 siRNA or negative control siRNA to BGI Japan. Data generated were in FASTQ format. RNA-seq reads were aligned to the human reference sequence and the gene annotations (UCSC hg19) using TopHat2 v2.0.14.[27] STAR v2.5.2a[28] was used to calculate FPKM values. Intron-retention-utils 0.5.1 was used to calculate intron retention events and the percent intron retention (PIR) of each gene.[29-31] PIR is calculated as the number of reads mapping to the 5′ and 3′ exon-intron junctions divided by the number of reads mapping exon-intron junctions plus any exon-exon junction that supports removal of that given intron.[32] RNA-seq results were visualized with the Broad Institute's Integrative Genomics Viewer (IGV) tool.[33]

2.17 | Gene set enrichment analysis

Associations between *DDX56* expression and previously defined gene sets were analyzed by gene set enrichment analysis (GSEA) using *DDX56* expression profiles from TCGA dataset.[34] Biologically defined gene sets were obtained from the Molecular Signatures Database v5.2 (http://software.broadinstitute.org/gsea/msigdb/index.jsp).

2.18 | Functional annotation and pathway enrichment analysis

Target genes derived from RNA-seq were grouped using Database for Annotation, Visualization and Integrated Discovery (DAVID v6.8; https://david.ncifcrf.gov) based on gene ontology (GO) for functional annotation of gene expression and pathway enrichment analysis based on the Kyoto Encyclopedia of Genes and Genomes (KEGG) database.[35] A cut off of P < .05 was used.

2.19 | Statistical analysis

Patient data from TCGA, Kyushu, and GSE datasets were divided into high *DDX56* mRNA expression and low *DDX56* mRNA expression groups using the minimum P-value approach.[36] Associations between variables were tested by Mann-Whitney U test, Student's t test, or Fisher's exact test. Overall survival (OS) curves were plotted according to the Kaplan-Meier method and compared using

TABLE 2 Univariate and multivariate analyses of clinicopathological factors affecting overall survival in CRC cases

Variable	HR	Univariate (95% CI)	P-value	HR	Multivariate (95% CI)	P-value
Age (≥65/<65 y)	1.54	(0.76-3.07)	.23			
Gender (male/female)	1.43	(0.69-3.25)	.36			
Tumor size (cm) (≥5/<5)	2.04	(1.23-4.11)	<.05	1.11	(0.53-2.42)	.77
Histological type (por, muc/well, mod)	6.40	(2.52-14.28)	<.01	3.46	(1.22-8.94)	<.05
T stage (3, 4/1, 2)	5.34	(1.90-22.27)	<.01	2.20	(0.61-10.43)	.24
Lymph node metastasis (+/−)	3.47	(1.69-7.64)	<.01	1.47	(0.57-3.88)	.43
Lymphatic invasion (+/−)	2.63	(1.31-5.44)	<.01	1.28	(0.54-3.10)	.58
Vascular invasion (+/−)	2.79	(1.38-5.55)	<.01	2.01	(0.95-4.22)	.07
Distant metastasis (+/−)	9.14	(4.28-18.88)	<.01	4.31	(1.76-10.76)	<.01
DDX56 expression (≥0.87/<0.87)	2.16	(1.07-4.62)	<.05	2.47	(1.08-6.02)	<.05

CI, confidential interval; CRC, colorectal carcinoma; HR, hazard ratio; mod, moderately differentiated adenocarcinoma; muc, mucinous adenocarcinoma; por, poorly differentiated adenocarcinoma; well, well-differentiated adenocarcinoma.

the log-rank test. Univariate and multivariate analyses were carried out using the Cox proportional hazards model to identify independent variables predictive of OS. Statistical analyses were done using JMP Pro 13 software (SAS Institute) and R v3.2.0 (The R Foundation for Statistical Computing). Statistical significance was set at $P \leq .05$.

3 | RESULTS

3.1 | DDX56 is a potential oncogene in CRC

DDX56 was selected as a potential oncogene using TCGA dataset through the screening described in Materials and Methods (Figure 1). RT-qPCR was used to compare *DDX56* mRNA expression in tumor tissues and normal colon tissues from 623 CRC patients in TCGA dataset and 108 CRC patients in the Kyushu dataset. *DDX56* mRNA expression was significantly higher in CRC tissues compared to normal colon tissues in TCGA and Kyushu datasets ($P < .05$) (Figure 2A). Increased DNA copy number of DDX56 (log2 copy number ratios >0.1) was observed in 384/613 (62.6%) of the CRC tissues.[37] Copy number of DDX56 was positively correlated with *DDX56* mRNA expression in TCGA dataset ($R = .67$, $P < .05$) (Figure 2B). Consistent with this, *DDX56* mRNA expression and DDX56 DNA copy number were positively correlated with CRC cell lines (Figure 2B). Frequency of mutations in *DDX56* was only 2.2% in TCGA dataset (Figure 2C). Immunohistochemical staining showed staining for DDX56 in tumor cells, and only weak to moderate

staining in non-cancerous colon cells (Figure 2D). Magnified images showed that DDX56 immunostaining was localized to the cytoplasm of tumor cells. Collectively, these results suggest that DDX56 is a potential oncogene induced by genomic amplification. Furthermore, this suggests that the amplification of DDX56 on Ch.7p is a fundamental and predominant event in the tumorigenesis of CRC.

3.2 | High DDX56 expression is correlated with lymphatic invasion and distant metastasis in CRC patients

Clinicopathological analysis showed that increased *DDX56* mRNA expression was correlated with lymphatic invasion ($P < .01$) and distant metastasis ($P < .05$) in the pathological, malignant CRC phenotype (Table 1). No difference in *DDX56* mRNA expression among stage I to IV tumors was observed in either TCGA or the Kyushu dataset (Figure S1).

3.3 | Increased DDX56 mRNA expression is correlated with poor survival in CRC patients

High *DDX56* mRNA expression groups had reduced OS compared to their respective low expression groups in the Kyushu, TCGA, and GSE datasets (Figure 2E). Furthermore, multivariate Cox regression analysis showed that high *DDX56* mRNA expression was an independent poor prognostic factor in the Kyushu dataset (HR = 2.47, 95% CI = 1.08-6.02, $P = .03$) (Table 2).

(A)

(B)

(C)

(D)

(E)

(F)

Days	6	7	9 *	13 *
NC (cm³)	0.04 ± 0.04	0.15 ± 0.16	0.44 ± 0.2	1.03 ± 0.46
shDDX56	0	0.05 ± 0.09	0	0.13 ± 0.08

(G)

(H)
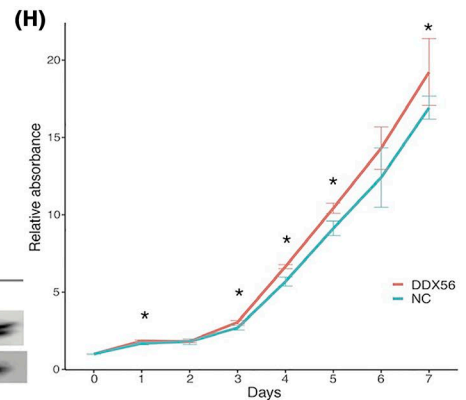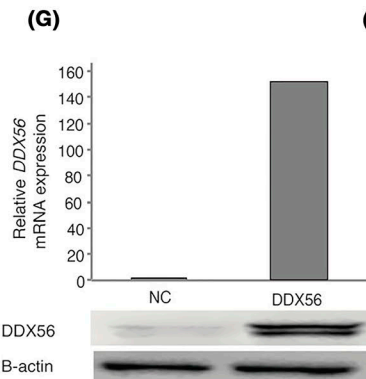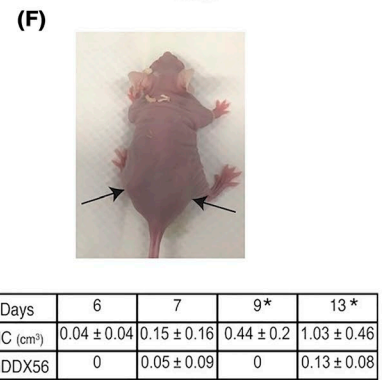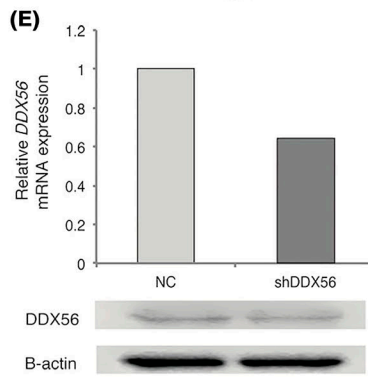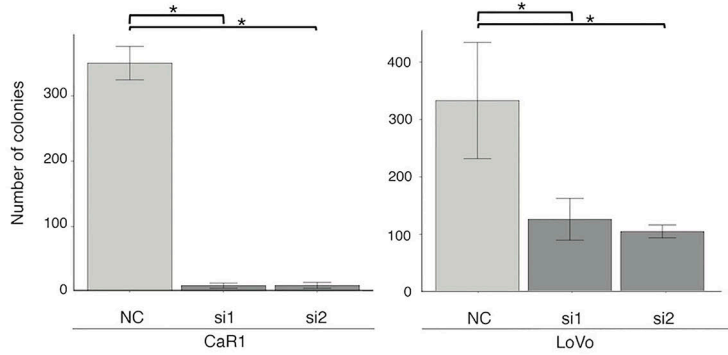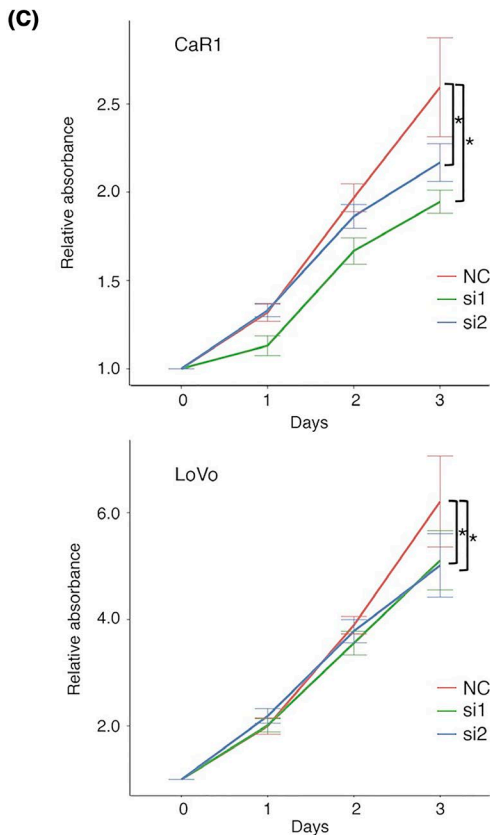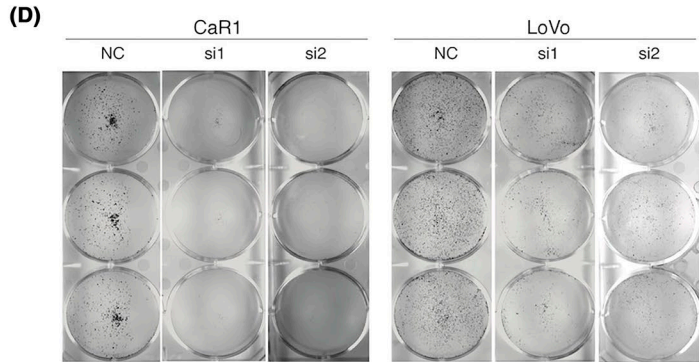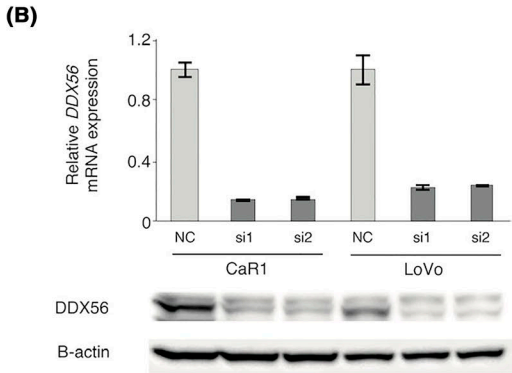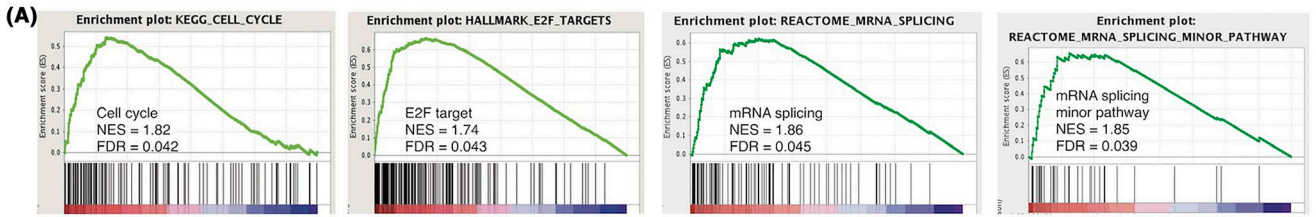
FIGURE 3 DDX56 is associated with cell growth of colorectal carcinoma. A, Gene Set Enrichment Analysis using The Cancer Genome Atlas (TCGA) dataset. B, *DDX56* mRNA expression using RT-qPCR and protein expression using western blot analysis in *DDX56* knockdown cells and control cells. C, MTT assays using DDX56-knockdown CaR1 and LoVo cells. *P < .05. D, Colony formation assays using DDX56-knockdown CaR1 and LoVo cells. NC, control, *P < .05. E, *DDX56* mRNA expression using RT-qPCR, and protein expression using western blot analysis in *DDX56* knockdown cells and control cells. F, In vivo analysis using a xenograft model. Tumor size in *DDX56* knockdown cells and control cells 9 d after s.c. injection. Arrow on right side of mouse points to *DDX56* knockdown cells and left side points to control cells. G, *DDX56* mRNA expression using RT-qPCR (upper panel) and protein expression using western blot analysis (lower panel) in *DDX56* overexpressed cells and control cells. H, MTT assay showing that *DDX56* overexpression significantly facilitated cell proliferation in SW480 cells. *P < .05. FDR, false discovery rate; NES, normalized enrichment score

3.4 | DDX56 expression is positively correlated with cell cycle and mRNA splicing pathways

To examine why increased *DDX56* mRNA expression may contribute to poor prognosis in CRC patients, GSEA of TCGA dataset was carried out. GSEA showed that overexpression of DDX56 was positively correlated with cell cycle and splicing-related pathways (Figure 3A).

3.5 | Knockdown of DDX56 inhibits cell proliferation and colony formation in CRC cell lines

Changes in the proliferation of CRC cell lines by *DDX56* knockdown were examined using MTT and colony formation assays. Knockdown of DDX56 decreased mRNA protein expression of DDX56 in CaR1 and LoVo cells (Figure 3B). MTT assays showed that *DDX56*
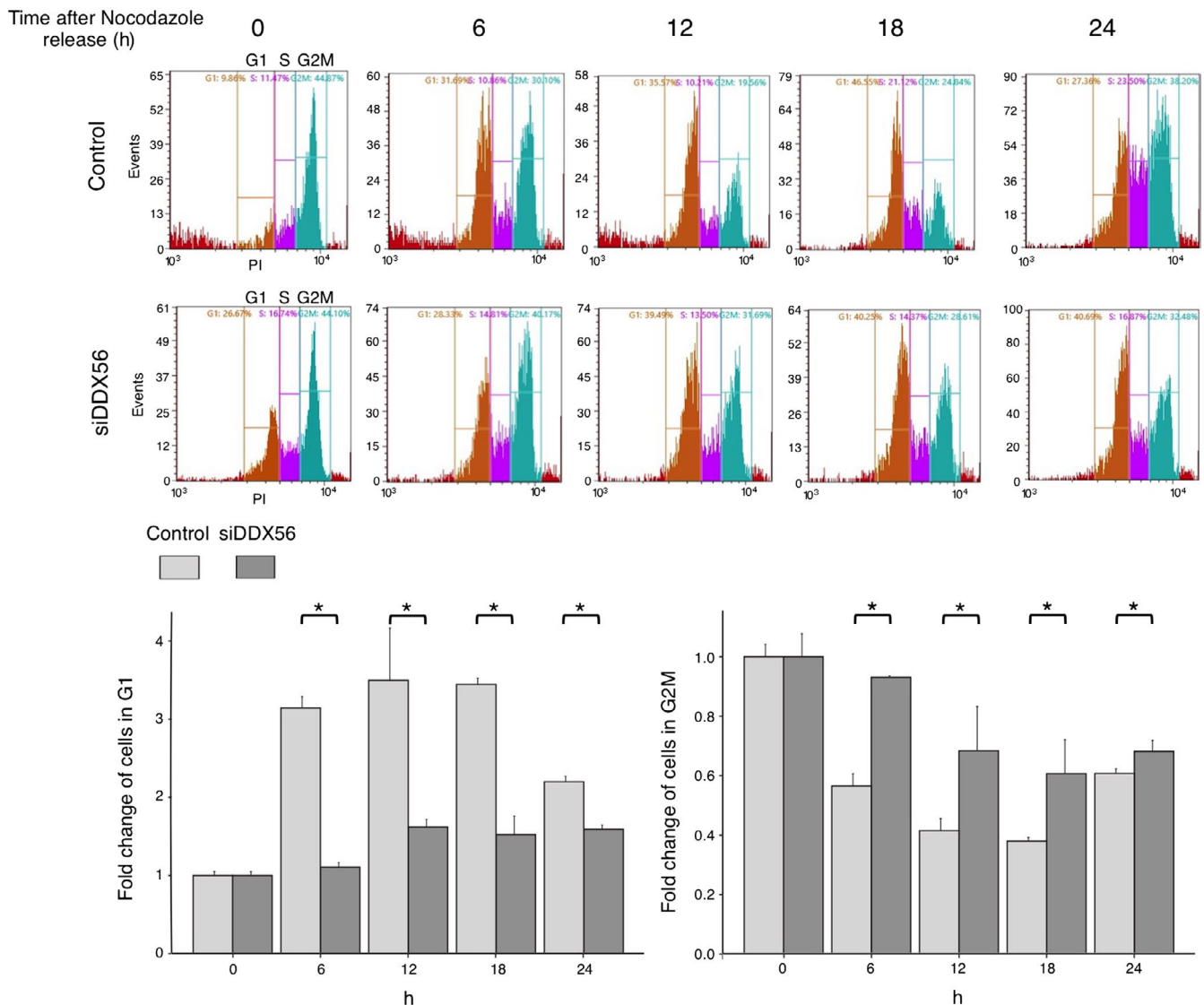
FIGURE 4 Knockdown of *DDX56* suspends cell cycle progression of colorectal carcinoma cells. Cell cycle assay after nocodazole release using FACS in control cells and *DDX56* knockdown cells. *P < .05

knockdown significantly suppressed cell proliferation in both CaR1 and LoVo cells (Figure 3C). Colony formation assay showed that *DDX56* knockdown significantly reduced colony formation in both CaR1 and LoVo cells (Figure 3D).

3.6 | Knockdown of *DDX56* inhibits tumor growth in a xenograft model

We conducted in vivo analysis using shRNA of *DDX56*. mRNA and protein expression of DDX56 were decreased in cells transfected with DDX56 shRNA (Figure 3E). Tumor size was larger in DDX56 shRNA cells than in control vector cells on days 9 and 13 after injection (Figure 3F).

3.7 | Overexpression of DDX56 facilitates cell proliferation

We used SW480 cells for overexpression analysis, because *DDX56* mRNA expression was lowest in SW480 cells among CRC cell lines (Figure S2). We transfected SW480 cells with *DDX56* expressing vector or empty vector. Overexpression of DDX56 increased mRNA and protein expression of DDX56 in SW480 cells (Figure 3G). MTT assays showed that *DDX56* overexpression significantly facilitated cell proliferation in SW480 cells (Figure 3H).

3.8 | Knockdown of DDX56 suspends cell cycle progression of CRC cell lines

DDX56 overexpression was positively correlated with cell cycle pathways using GSEA (Figure 3A). To examine the role of *DDX56* expression in cell cycle progression, cell cycle assay of siDDX56-transfected CaR1 cells using FACS was conducted. Distribution of cells in G1 phase and G2M phase was higher and lower, respectively, in control cells compared to *DDX56* knockdown cells at 6-24 hours after nocodazole treatment (Figure 4). These results indicate that knockdown of DDX56 can suspend cell cycle progression from G2M to G1 phase in a CRC cell line.

These results suggest that DDX56 overexpression facilitates cell growth in CRC by cell cycle progression.

3.9 | Knockdown of DDX56 suppresses intron retention in cell cycle-related genes

Several DEAD-Box proteins are reported to be involved in mRNA splicing. GSEA also indicated that DDX56 has a role in mRNA splicing. To assess the involvement of DDX56 in mRNA splicing, RNA-seq

of CRC cell lines transfected with siDDX56 was carried out. Notably, knockdown of DDX56 was associated with a reduction in PIR at 1915 intron positions in 753 genes (fold change <0.5) (Figure 5A). DAVID analysis showed that many of the 753 affected genes were related to cell cycle, cell division, and mitosis pathways (Figure 5B). Among 753 genes, 58 genes including WEE1 were related to cell cycle pathways, and knockfown of DDX56 led to a reduction on PIR in these 58 genes (Figure 5C), knockdown of DDX56 led to a reduction in PIR. WEE1, which plays a crucial role in the G2-M cell cycle checkpoint, is reported to have a tumor-suppressive role and suppressed expression in colon cancer.[38] To validate the results of RNA-seq, RT-qPCR of the retained WEE1 intron in si*DDX56*-transfected cells was carried out. Consistent with the results of RNA-seq, expression of the retained *WEE1* intron was higher in control cells compared to cells transfected with siDDX56 (Figure 5D). These results indicate that knockdown of DDX56 induces intron reduction in cell cycle-related genes, including WEE1.

3.10 | Knockdown of DDX56 increases wild-type WEE1 expression

Western blot analysis was done using anti-WEE1 N-terminal antibody to confirm the protein expression of WEE1 and the effect of intron retention. Figure 5E shows the position of the retained intron in *WEE1* and the expected molecular weight of WEE1 protein. Intron retention was expected to lead to mutations at the 3′ terminus of WEE1 and a consequent truncated WEE1 protein as a result of a new stop codon. Wild-type WEE1 protein weight is 72.5 kDa. The expected truncated WEEI protein weight was 42.5 kDa. The truncated WEE1 protein was too small to detect in knockdown and control cells. However, wild-type WEE1 protein expression was higher in siDDX56-transfected cells compared to control cells, indicating that knockdown of DDX56 decreased intron retention in *WEE1* and increased wild-type WEE1 protein expression (Figure 5F). These findings suggest that DDX56 can induce intron retention in WEEI, which produces a consequent truncated WEE1 protein that does not function as a tumor suppressor.

3.11 | WEE1 intron (truncated WEE1) mRNA expression in the DDX56 high group is higher than in the DD56 low group of CRC patients

To determine the clinical significance of WEE1 intron retention (truncated WEE1), expression of the WEE1 intron in the Kyushu dataset was investigated by RT-qPCR. Truncated WEE1 mRNA expression was compared between the DDX56 high group and the

---

FIGURE 5 Knockdown of *DDX56* suppressed intron retention in cell cycle-related genes including tumor suppressor *WEE1*. A, Number of positions and fold change (knockdown/control) of percent intron retention in *DDX56* knockdown and normal control cells. B, Pathways of intron-retained genes in *DDX56* knockdown cells vs control cells using DAVID. C, Rate of intron retention of genes in cell cycle pathways. D, Expression of *WEE1* intron using RT-qPCR. *P < .05. E, Expected mRNA and predicted protein weight of WEE1. Blue bar indicates the retained intron that contained a stop codon. F, Western blot analysis of WEE1. *P < .05. G, *WEE1* intron RNA expression in the Kyushu dataset. *P < .05. H, *WEE1* intron RNA expression in TCGA dataset and Kyushu dataset. *P < .05

(A) Fold change ≦1/2 in two cell lines 1915 positions 753 genes

(B) −log10 (FDR) in DAVID

(C)

(D)

(E) WEE1 hg19

(F)

(G) Kyushu dataset

(H) TCGA dataset · Kyushu dataset
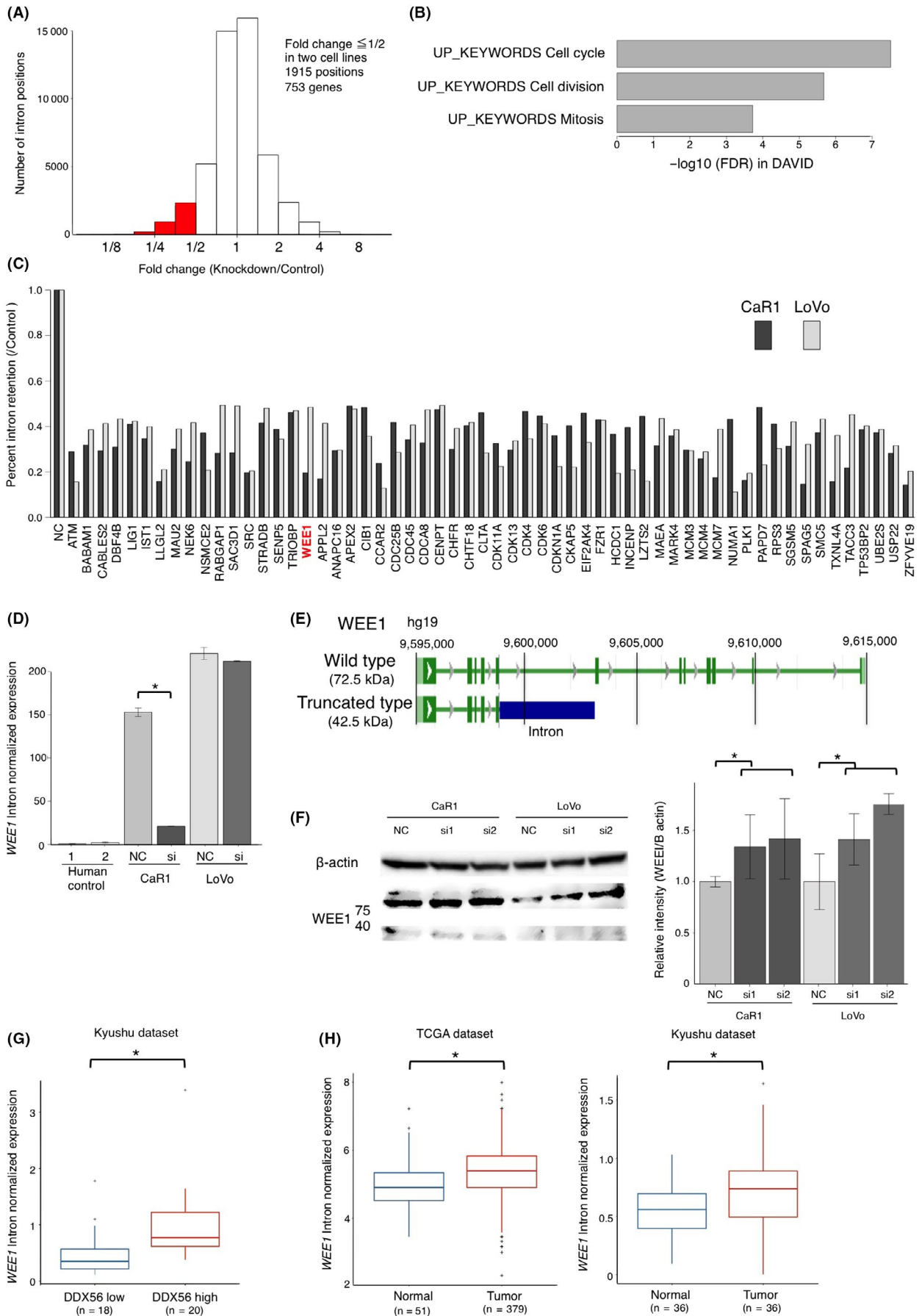
DDX56 low group. As expected, truncated WEE1 mRNA expression in the *DDX56* high group was higher than in the DDX56 low group of CRC patients (Figure 5G).

3.12 | WEE1 intron (truncated WEE1) mRNA expression in tumor tissues is higher than in normal tissues

Expression of *WEE1* intron mRNA in CRC tissues was higher than in normal tissues in TCGA and Kyushu dataset ($P < .05$) (Figure 5H). These observations further indicate that the tumor suppressor WEE1 is suppressed by mRNA splicing abnormalities in CRC.

3.13 | DDX56 is overexpressed in various cancers

Expression of *DDX56* mRNA in various cancer types and normal tissues was compared using TCGA dataset. Expression of *DDX56* mRNA was higher in nine different cancer tissues, as well as CRC, compared to *DDX56* mRNA expression in respective non-cancerous tissues (Figure S3). This result indicates that DDX56 may be a common driver gene in various cancers.

4 | DISCUSSION

In the present study, we showed that *DDX56* is amplified in CRC and that high expression of *DDX56* leads to a poor prognosis. Furthermore, we showed that DDX56 could promote cell proliferation by inducing oncogenic splicing alteration in a cell cycle checkpoint gene, *WEE1*. To the best of our knowledge, this is the first study to explore the function of DDX56 as an oncogenic driver and prognostic biomarker of CRC.

DDX56 is a member of the DDX family of proteins that make up the largest RNA helicase family and are characterized by the presence of an Asp-Glu-Ala-Asp (DEAD) motif. Several DDX family members play roles in alternative splicing.[18,19] DDX5 and DDX17 contribute to tumor-cell invasiveness by regulating alternative splicing of several DNA- and chromatin-binding factors.[3] Although DDX56 is reported to be required in West Nile virus infection,[39] the relationship of DDX56 with malignancies remains unknown. Our clinical analysis showed that *DDX56* on Ch.7p is amplified in CRC, and overexpression is associated with malignant, pathological phenotypes, such as lymphatic invasion and distant metastasis. Notably, *DDX56* overexpression was an independent prognostic factor in CRC. In our experimental analysis, we found that DDX56 promotes cell proliferation by facilitating cell cycle progression, possibly by inducing splicing alteration in tumor suppressor *WEE1*. Furthermore, *DDX56* is overexpressed in various cancers. These findings provide clinical and biological evidence that *DDX56* is a novel oncogene in CRC, and may function as a driver gene in various cancers in addition to CRC.

WEE1 is a tyrosine kinase that is a crucial component of the G2-M cell cycle checkpoint, preventing entry into mitosis in response to cellular DNA damage, and plays a tumor-suppressive role.[40] The expression of WEE1 is suppressed in colon cancer and non-small cell lung cancer.[38,41] Interestingly, the expression of some tumor suppressor genes, such as *LKB1* and *KLF6*, was controlled by splicing alterations.[2,6,42] In the present study, we showed that *WEE1* expression is also altered through alternative splicing by *DDX56* overexpression. RNA sequence analysis showed that knockdown of *DDX56* immediately reduced the intron retention of *WEE1* (truncated WEE1) and increased wild-type *WEE1* mRNA expression. Furthermore, our clinical analysis showed that the expression of truncated WEE1 in CRC tissues was higher than in normal tissues and that the expression of truncated WEE1 was higher in a high DDX56 expression cohort compared with a low DDX56 expression cohort of CRC patients. These findings indicate that *WEE1* expression could be suppressed by alternative splicing induced by the overexpression of DDX56. WEE1 suppression likely promotes cell cycle progression and the consequent cell proliferation of CRC, leading to the poor prognosis of CRC patients (Figure 6).

The mechanism by which DDX56 induces abnormal splicing of *WEE1* is unknown. Alternative splicing by DDX family members is reported to alter a functional spliceosome assembly.[19] Because DDX56 shares common structures with the DDX family members,[18] DDX56 may also change splicing by spliceosome assembly alteration.
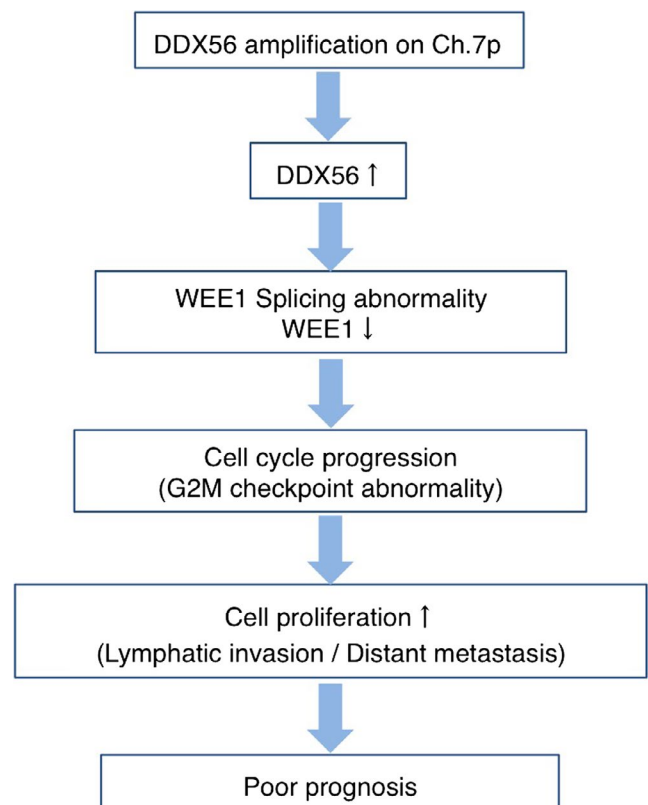
FIGURE 6 Summary of results. Amplification of *DDX56* on Ch. 7p induced high expression of *DDX56*. High expression of *DDX56* altered the splicing of the cell cycle-related gene, *WEE1*, and led to cell cycle progression, which contributes to cell proliferation and poor prognosis in colorectal carcinoma

Further study will be required to clarify the mechanism of DDX56 on alternative splicing in malignant cancers.

In conclusion, we have identified a novel oncogene, *DDX56*, on Ch.7p that promotes alternative splicing of the tumor suppressor gene, *WEE1*, and provided evidence that DDX56 may be a potential therapeutic target to overcome intratumor heterogeneity in CRC.

DISCLOSURE

Authors declare no conflicts of interest for this article.

ORCID

Koshi Mimori https://orcid.org/0000-0003-3897-9974

REFERENCES

1. Yoshida K, Ogawa S. Splicing factor mutations and cancer. *Wiley Interdiscip Rev RNA*. 2014;5(4):445-459.
2. Srebrow A, Kornblihtt AR. The connection between splicing and cancer. *J Cell Sci*. 2006;119(Pt 13):2635-2641.
3. Dardenne E, Pierredon S, Driouch K, et al. Splicing switch of an epigenetic regulator by RNA helicases promotes tumor-cell invasiveness. *Nat Struct Mol Biol*. 2012;19(11):1139-1146.
4. Yoshida K, Sanada M, Shiraishi Y, et al. Frequent pathway mutations of splicing machinery in myelodysplasia. *Nature*. 2011;478(7367):64-69.
5. Zhang J, Lieu YK, Ali AM, et al. Disease-associated mutation in SRSF2 misregulates splicing by altering RNA-binding affinities. *Proc Natl Acad Sci USA*. 2015;112(34):E4726-E4734.
6. Seiler M, Peng S, Agrawal AA, et al. Somatic mutational landscape of splicing factor genes and their functional consequences across 33 cancer types. *Cell Rep*. 2018;23(1):282-296.e284.
7. Silipo M, Gautrey H, Tyson-Capper A. Deregulation of splicing factors and breast cancer development. *J Mol Cell Biol*. 2015;7(5):388-401.
8. Chen J, Weiss WA. Alternative splicing in cancer: implications for biology and therapy. *Oncogene*. 2015;34(1):1-14.
9. Bisognin A, Pizzini S, Perilli L, et al. An integrative framework identifies alternative splicing events in colorectal cancer development. *Mol Oncol*. 2014;8(1):129-141.
10. Lee AR, Gan Y, Xie N, Ramnarine VR, Lovnicki JM, Dong X. Alternative RNA splicing of the GIT1 gene is associated with neuroendocrine prostate cancer. *Cancer Sci*. 2019;110:245-255.
11. Sato K, Masuda T, Hu Q, et al. Phosphoserine phosphatase is a novel prognostic biomarker on chromosome 7 in colorectal cancer. *Anticancer Res*. 2017;37(5):2365-2371.
12. Herbergs J, Arends JW, Bongers EM, Ramaekers FC, Hopman AH. Clonal origin of trisomy for chromosome 7 in the epithelial compartment of colon neoplasia. *Genes Chromosom Cancer*. 1996;16(2):106-112.
13. Zarzour P, Boelen L, Luciani F, et al. Single nucleotide polymorphism array profiling identifies distinct chromosomal aberration patterns across colorectal adenomas and carcinomas. *Genes Chromosom Cancer*. 2015;54(5):303-314.
14. Uchi R, Takahashi Y, Niida A, et al. Integrated multiregional analysis proposing a new model of colorectal cancer evolution. *PLoS Genet*. 2016;12(2):e1005778.
15. Saito T, Niida A, Uchi R, et al. A temporal shift of the evolutionary principle shaping intratumor heterogeneity in colorectal cancer. *Nat Commun*. 2018;9(1):2884.
16. Niida A, Nagayama S, Miyano S, Mimori K. Understanding intratumor heterogeneity by combining genome analysis and mathematical modeling. *Cancer Sci*. 2018;109(4):884-892.
17. Bedard PL, Hansen AR, Ratain MJ, Siu LL. Tumour heterogeneity in the clinic. *Nature*. 2013;501(7467):355-364.
18. Linder P, Jankowsky E. From unwinding to clamping – the DEAD box RNA helicase family. *Nat Rev Mol Cell Biol*. 2011;12(8):505-516.
19. Bourgeois CF, Mortreux F, Auboeuf D. The multiple functions of RNA helicases as drivers and regulators of gene expression. *Nat Rev Mol Cell Biol*. 2016;17(7):426-438.
20. Tanaka K, Ikeda N, Miyashita K, Nuriya H, Hara T. DEAD box protein DDX1 promotes colorectal tumorigenesis through transcriptional activation of the LGR5 gene. *Cancer Sci*. 2018;109(8):2479-2489.
21. Watanabe T, Itabashi M, Shimada Y, et al. Japanese Society for Cancer of the Colon and Rectum (JSCCR) guidelines 2010 for the treatment of colorectal cancer. *Int J Clin Oncol*. 2012;17(1):1-29.
22. Ueda M, Iguchi T, Nambara S, et al. Overexpression of transcription termination factor 1 is associated with a poor prognosis in patients with colorectal cancer. *Ann Surg Oncol*. 2015;22(suppl 3):S1490-S1498.
23. Sato K, Masuda T, Hu Q, et al. Novel oncogene 5MP1 reprograms c-Myc translation initiation to drive malignant phenotypes in colorectal cancer. *EBioMedicine*. 2019;44:387-402.
24. Kurashige J, Hasegawa T, Niida A, et al. Integrated molecular profiling of human gastric cancer identifies DDR2 as a potential regulator of peritoneal dissemination. *Sci Rep*. 2016;6:22371.
25. Liu R, Li J, Zhang T, et al. Itraconazole suppresses the growth of glioblastoma through induction of autophagy: involvement of abnormal cholesterol trafficking. *Autophagy*. 2014;10(7):1241-1255.
26. Kawasaki Y, Komiya M, Matsumura K, et al. MYU, a target lncRNA for Wnt/c-Myc signaling, mediates induction of CDK6 to promote cell cycle progression. *Cell Rep*. 2016;16(10):2554-2564.
27. Trapnell C, Roberts A, Goff L, et al. Differential gene and transcript expression analysis of RNA-seq experiments with TopHat and Cufflinks. *Nat Protoc*. 2012;7(3):562-578.
28. Dobin A, Davis CA, Schlesinger F, et al. STAR: ultrafast universal RNA-seq aligner. *Bioinformatics*. 2013;29(1):15-21.
29. Braunschweig U, Barbosa-Morais NL, Pan Q, et al. Widespread intron retention in mammals functionally tunes transcriptomes. *Genome Res*. 2014;24(11):1774-1786.

30. Jung H, Lee D, Lee J, et al. Intron retention is a widespread mechanism of tumor-suppressor inactivation. *Nat Genet*. 2015;47(11):1242-1248.

31. Dobin A, Gingeras TR. Mapping RNA-seq reads with STAR. *Curr Protoc Bioinformatics*. 2015;51:11.14-11.19.

32. Fernandez JP, Moreno-Mateos MA, Gohr A, et al. RES complex is associated with intron definition and required for zebrafish early embryogenesis. *PLoS Genet*. 2018;14(7):e1007473.

33. Robinson JT, Thorvaldsdottir H, Winckler W, et al. Integrative genomics viewer. *Nat Biotechnol*. 2011;29(1):24-26.

34. Subramanian A, Tamayo P, Mootha VK, et al. Gene set enrichment analysis: a knowledge-based approach for interpreting genome-wide expression profiles. *Proc Natl Acad Sci USA*. 2005;102(43):15545-15550.

35. Huang da W, Sherman BT, Lempicki RA. Systematic and integrative analysis of large gene lists using DAVID bioinformatics resources. *Nat Protoc*. 2009;4(1):44-57.

36. Mizuno H, Kitada K, Nakai K, Sarai A. PrognoScan: a new database for meta-analysis of the prognostic value of genes. *BMC Med Genomics*. 2009;2:18.

37. Beroukhim R, Getz G, Nghiemphu L, et al. Assessing the significance of chromosomal aberrations in cancer: methodology and application to glioma. *Proc Natl Acad Sci USA*. 2007;104(50):20007-20012.

38. Backert S, Gelos M, Kobalz U, et al. Differential gene expression in colon carcinoma cells and tissues detected with a cDNA array. *Int J Cancer*. 1999;82(6):868-874.

39. Reid CR, Hobman TC. The nucleolar helicase DDX56 redistributes to West Nile virus assembly sites. *Virology*. 2017;500:169-177.

40. Kawabe T. G2 checkpoint abrogators as anticancer drugs. *Mol Cancer Ther*. 2004;3(4):513-519.

41. Yoshida T, Tanaka S, Mogi A, Shitara Y, Kuwano H. The clinical significance of Cyclin B1 and Wee1 expression in non-small-cell lung cancer. *Ann Oncol*. 2004;15(2):252-256.

42. Miller J, Dreyer TF, Bacher AS, et al. Differential tumor biological role of the tumor suppressor KAI1 and its splice variant in human breast cancer cells. *Oncotarget*. 2018;9(5):6369-6390.

SUPPORTING INFORMATION

Additional supporting information may be found online in the Supporting Information section at the end of the article.